Effects of Finite Layer Thickness on the Differential Capacitance of Electron Bilayers

J.J. Durrant: McNair Scholar

Dr. Charles Hanna: Mentor

Physics

Abstract

We have calculated the effects of finite thickness on electron or hole layers in double-quantum-well systems. In particular, we apply our model to calculate the Eisenstein ratio and the interlayer capacitance of a biased bilayer device; these are direct measures of the compressibility of the charge carriers in the layers. We show that our model agrees well with the experimental layer-occupancy data for a device of this type. We present results for the regime of negligible interlayer tunneling, zero applied magnetic field, and low layer densities, when the compressibility of one or both layers is negative.

Introduction

In this paper, we extend models of double-quantum-well electron or hole systems that have front and back gates and separately contactable layers to include finite-thickness effects. Previous theoretical models[1-4] have modeled the charge density in the quantum wells as two-dimensional electron gases (2DEGs). However, while the 2DEG model is an effective one,[1, 2, 5, 6] it is also an idealized approximation, since the quantum-well confining potential of the 2DEG has a finite thickness, usually on the order of 15 nm.[5] In this paper, we incorporate the effects of this finite-thickness by allowing the charges to have an additional spatial degree of freedom normal to the plane where the 2DEG is confined. Our approach is to derive the corrections to the 2DEG model based on the consequences of including this additional degree of freedom.

We present a pictorial overview of our model of a double-quantum-well system as follows. Figure 1 (below) shows the geometry of the device. The front (F) and back (B) gates are distances D_F and D_B from the two quantum wells, labeled 1 and 2, respectively. The two quantum wells are separated by an interlayer distance d. Typically, real devices have dimensions on the order of $D_B \sim 3\ \mu$m, $D_F \sim 0.3\ \mu$m, and $d \sim 15$ nm. The gates and layers are charged by the application of the front-gate voltage V_F (between the front gate and layer 1) and the back-gate voltage V_B (between the back gate and layer 2). If the layers are separately contactable, then a middle voltage V_M can be maintained between the layers, otherwise the layers share a common ground.

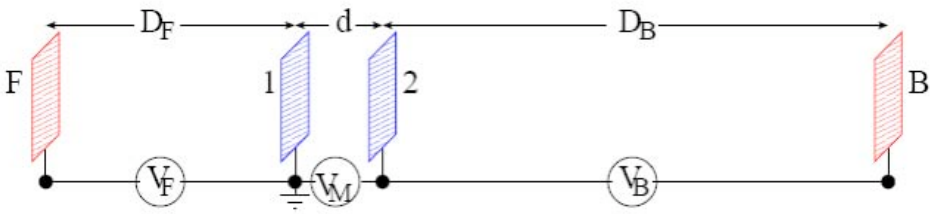

Figure 1. Schematic illustration of a double-quantum-well device with front (F) and back (B) gates, two quantum wells (layers 1 and 2), and front-gate, middle (interlayer), and back-gate voltages V_F, V_M, and V_B, respectively. The distances D_F, d, and D_B are the separations between the front gate and layer 1, layer 1 and layer 2, and layer 2 and the back gate, respectively.

Figure 2 (below) shows the electric fields produced by the charges on the gates and layers of the device. Earlier models treated the charges densities in the quantum wells (layers 1 and 2) as two dimensional,[2-4] but here we will focus on finite-thickness corrections to the two-dimensional models. The surface charge densities on the front and back gates are denoted by en_F and en_B, respectively, and the surface charges densities on the layers are denoted

by $-en_1$ and $-en_2$, respectively, where e is the charge of an electron. Note that in a hole (p-type) system, the signs of the charges in the gates and layers reverse sign. A system of this type will be discussed in Section 3. The electric fields produced by the charges are denoted by $\vec{E}_F$ (between the front gate and layer 1), $\vec{E}_M$ (between layer 1 and layer 2), and $\vec{E}_B$ (between layer 1 and the back gate). Since the area of the gates and layers is on the order of 1 mm, [2] while the separations between the layers are on the order of at most 10 μm, we approximate the electric fields as uniform.[7]

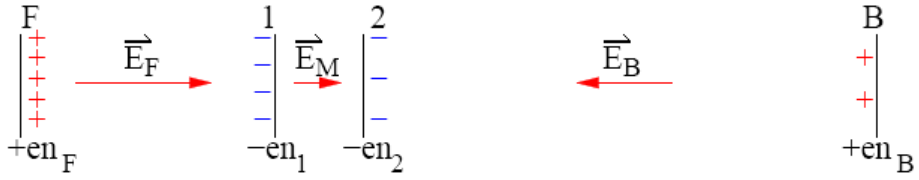

Figure 2. Electrical charges on the gates and layers produce electric fields $\vec{E}_F$, $\vec{E}_M$, and $\vec{E}_B$, between the gates and layers, shown for electron (n-type) bilayers.

Having defined the parameters relevant to our model, we proceed to proceed to derive corrections to the 2DEG model based on finite-thickness effects in Section 2. We apply our model by calculating a theoretical fit to an experiment with a double-quantum-well device[5] in Section 3. We also calculate the Eisenstein ratio[2, 4] and the interlayer capacitance between layer 1 and layer 2 for this same device in Section 3. Finally, we discuss the implications of our results in Section 4.

Theoretical Model

In this section, we develop a theoretical model to describe the behavior of double-quantum-well devices. Our task is to extend two-dimensional models, derived by previous workers[2-4], to include the effects of finite thickness. We present corrections based on finite-thickness to the expression for energy per area of a double layer system. From this result, we derive corrections to the chemical potential and the density of states. For simplicity, we assume that the charges carriers in both layers have no net spin polarization.

Our first consideration is the energy per area U of a single layer of electrons (holes) in a double-quantum-well system. We can express this quantity as the sum of two terms

$$U = U_{\mathrm{C}} + U_{\mathrm{QM}}, \tag{1}$$

where U_{C} is the energy *per area* due to classical electrostatic interactions, and U_{QM} contains both the energy per area arising from the quantum-mechanical exchange energy, and the kinetic energy per area of the electron (hole) gas. By assuming a 2DEG model -- i.e., that each layer has zero thickness -- expressions for U_{C} and U_{QM} have been derived[3, 4, 8] that agree well with experiments.[2, 6] In the 2DEG model, these expressions are

$$U_{\mathrm{C}} = \frac{e^2}{4\pi\varepsilon}\left(n_F - n_1\right)^2 d \tag{2}$$

and, in the Hartree-Fock approximation,[4]

$$U_{\mathrm{QM}} = \frac{\pi\hbar^2}{2m^*}n^2 - \frac{8/3}{\sqrt{2\pi}}\frac{e^2}{4\pi\varepsilon}n^{3/2}, \tag{3}$$

where d is the effective separation between the 2DEGs, m^* is the effective mass of the electrons (holes), and ε is the dielectric constant of the semiconductor host. We also assume that each layer is independent of each other (no interlayer coherence); i.e., that $U(n_1, n_2) = U(n_1) + U(n_2)$.

The previous results are all obtained under the assumption of two-dimensional layer densities. We now derive corrections to Eq. (2) and Eq. (3) to include an additional degree of freedom normal to the plane of the 2DEGs; i.e., we allow the 2DEGs to have some finite-thickness within the quantum wells. For a single layer of density n, the correction to U_{QM}, which we call δU_{QM}, is given by[7, 9]

$$\delta U_{\mathrm{QM}} = -\frac{8/3}{\sqrt{2\pi}}\frac{e^2}{4\pi\varepsilon}n^{3/2}\left[G\left(k\right)-1\right], \tag{4}$$

where $k = 2(\pi n)^{1/2}$ is the Fermi wave vector, and

$$G\left(k\right) = \frac{3}{2}\int_0^1 dx\, F\left(kx\right)\left[\pi/2 - \sin^{-1}\left(x\right) - x\sqrt{1-x^2}\right]. \tag{5}$$

Here $F(k)$ is the "form factor," which depends on the envelope wave function $\zeta(z)$ that describes the density profile of the charges in the well,[9, 10] via

$$F(k) = \int dz \int dz' e^{-k|z-z'|}\left|\zeta\left(z-d\right)\right|^2\left|\zeta\left(z'-d\right)\right|^2, \tag{6}$$

where $\zeta(z)$ is the density-profile wave function of the well. Note that in the zero-thickness limit $|\zeta(z\text{-}d)|^2 \rightarrow \delta(z\text{-}d)$, and $F(k)\rightarrow 1$, so that δU_{QM} vanishes and we obtain the 2DEG result. Using these results, it can be shown that the correction to the to U_C, which we call δU_C, is given by

$$\delta U_{\mathrm{C}} = \frac{e^2\bar{n}^2}{2}\lim_{k\to 0}\left[\frac{\partial}{\partial k}F\left(k\right)\right] \equiv -\frac{e^2\bar{n}^2}{\varepsilon}w, \tag{7}$$

from which we define the thickness w as

$$w \equiv -\lim_{k\to 0}\left[\frac{\partial}{\partial k}F\left(k\right)\right]. \tag{8}$$

We can now calculate the effects of finite-thickness based from the corrections expressed in Eq. (4) and Eq. (7), which is the topic of the next section. To calculate quantities of interests, we will also need the first and second derivatives of U with respect to layer density n, which are the layer chemical potential μ, defined as[3]

$$\mu = \frac{\partial}{\partial n}U_{\mathrm{QM}}, \tag{9}$$

and the thermodynamic length s, which is proportional to the density of states, and defined by

$$s = \frac{\varepsilon}{e^2}\frac{\partial\mu}{\partial n} = \frac{\varepsilon}{e^2\bar{n}^2\kappa}, \tag{10}$$

where κ is the electron compressibility. At low densities ($n\rightarrow 0$), the electronic compressibility becomes negative,[2-4] which implies that

$$\lim_{n \to 0} s(n) \to -\infty . \tag{11}$$

From Eq. (9) and Eq. (10), the finite-thickness corrections to μ and s, denoted by $\delta\mu$ and δs, respectively, are calculated to be

$$\delta\mu = -\frac{e^2 n}{\varepsilon} w + \frac{\delta U_{\mathrm{QM}}}{n_{js}} + \frac{4e^2}{\varepsilon}\sqrt{\frac{n}{\pi}}\left[\frac{1}{3} - \int_0^1 dx\, F(kx)\, x\sqrt{1-x^2}\right], \tag{12}$$

$$\delta s = -w + \frac{2}{\sqrt{\pi n}}\left[1 - \int_0^1 dx\, F(kx)\frac{x}{\sqrt{1-x^2}}\right]. \tag{13}$$

We are now in position to calculate the effects on finite thickness, based on the corrections to the energy per unit area, the chemical potential, and the thermodynamic length. These calculations are the topic of the next section.

Results

In this section, we present some calculations based on the model developed in the previous sections. First, we discuss the assumptions used in our calculations. Second, we present a theoretical fit to an experiment conducted with a double-quantum-well device. Third, we present a calculation of the Eisenstein ratio. Finally, we present a calculation of the interlayer capacitance.

As discussed in the previous section, the finite-thickness corrections to the energy per area depend on the form factor $F(k)$, given in Eq. (6). For simplicity, we choose the ground-state infinite-square-well wave function for $\zeta(z)$, given by

$$\zeta(z) = \sqrt{\frac{2}{b}}\cos\left(\frac{\pi z}{b}\right), \tag{14}$$

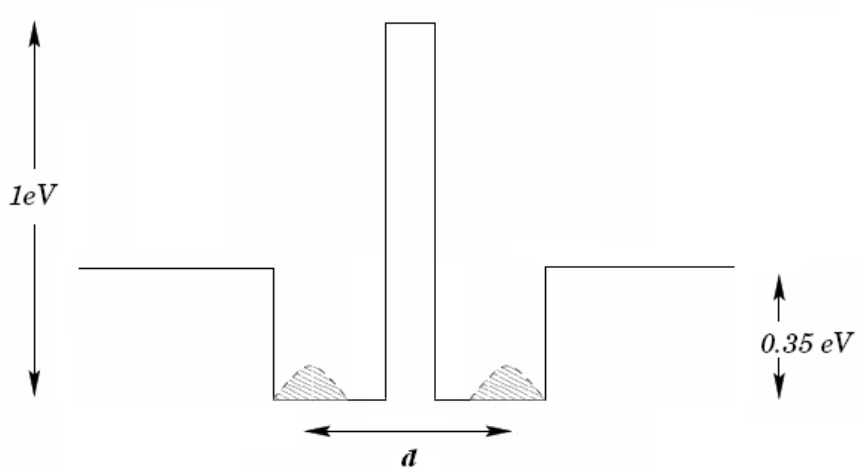

Figure 3. Pictorial overview of our approach to choosing a form factor for our model. The figure shows two quantum wells, with outer barriers of ~ 0.35 eV and an inner barrier of ~ 1 eV. Two infinite-square-well ground state wave functions occupy the wells, and their width is allowed to vary the full thickness of the well, subject to the constraint that the outer nodes of the wave functions must be located at the outer 0.35 eV barriers.

where b is the "width" of the wave function. Using Eq. (6), the form factor is calculated to be[9]

$$F(k)=\left[2\left(\frac{bk}{(bk)^2+(2\pi)^2}-\frac{1}{bk}\right)^2\left(e^{-bk}-1\right)+\frac{2}{bk}+\frac{bk}{(bk)^2+(2\pi)^2}\right]. \tag{15}$$

Note that in the zero-thickness limit $b\to 0$, one obtains $F(k)\to 1$; the finite-thickness corrections vanish, and we obtain the 2DEG model. Using Eq. (15) as our expression for the form factor, we can now calculate the energy *per area* of a double-quantum-well system, using Eq. (2), and adding in the finite-thickness corrections, Eqs. (4) and (7). We minimize the expression for the energy per area using a variational approach, under the following constraints, which are summarized pictorially in Figure 3 (above). The minimization is done with respect to the population of the first layer n_1, and the separation between the layers d is left as a free fitting parameter. The value n_1 constrains the value for n_2 since the total charge of the layers n_T is known and is given by $n_T = n_1 + n_2$, up to an overall constant. The constraint that the wave function be pinned to the outside of the well (see Figure 3) may be expressed as

$$d = 2a - b, \tag{16}$$

where a is the distance from the middle of the barrier separating the wells to the outer barrier of one of the wells, and b is the width parameter in Eq. (14). Eq (16) forces the wave function to vanish at the outer barrier, and allows the width b of the wave function to vary from zero up to the width of the well. The precise value of b is determined by choosing an appropriate d to fit experimental data. It follows from Eq. (8) that

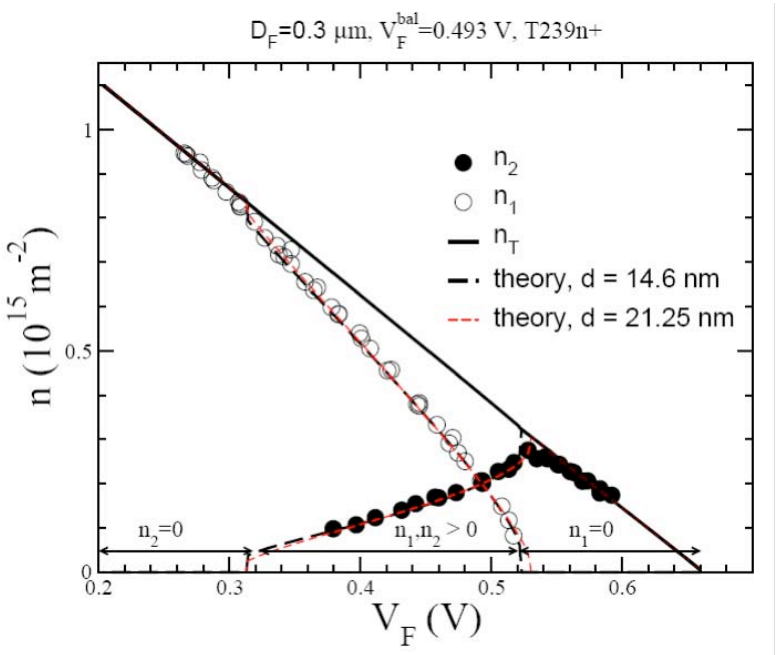

Figure 4. Layers densities versus front-gate voltage V_F for the bilayer sample of Ref.
The figure shows both the theoretical fits, with and without finite-thickness effects. The fit gives a larger effective interlayer separation (d = 21.25 nm) when finite-thickness affects are included, and improves the agreement with experiment at the bilayer-monolayer transition.

$$w=-\lim_{k\to 0}\left[\frac{\partial}{\partial k}F(k)\right]=\left(\frac{12\pi^2}{4\pi^2-15}\right)b. \tag{17}$$

Figure 4 (above) shows data from Ref. 5. The figure shows an exchange-driven monolayer-bilayer-monolayer transition with increasing total density (decreasing V_F) in a *p*-type (hole) system. Using our variational approach, we minimized the energy per area to find n_1 and n_2 as a function of the front-gate voltage V_F, and chose d to fit the data. A value of d = 14.6 nm gave the best fit for the 2DEG model, while d = 21.25 nm gave the best fit when finite-thickness corrections were included. Choosing d = 21.25 nm gives b = 8.7 nm, meaning that the wave function occupies 58% of a 15 nm wide well. Both models offer excellent agreement with the experimental data, with the finite-thickness corrections improving the agreement somewhat. Note that the 2DEG model overestimates the abruptness of the bilayer-to-monolayer transition,[6] and that the finite-thickness corrections improve the agreement by softening this abrupt transition.

Another quantity of interest that can be experimentally measured is the Eisenstein ratio R_E.[1, 2] The Eisenstein ratio is defined as[4]

$$R_E \equiv \frac{\delta E_M}{\delta E_F} = 1 - \frac{\delta n_1}{\delta n_F}, \tag{18}$$

where δE_F is the differential change in eletric field between the front-gate and layer 1, δE_M is the differential change in electric field between layer 1 and layer 2, and δn_1 and δn_F are the differential changes in charge on the first layer

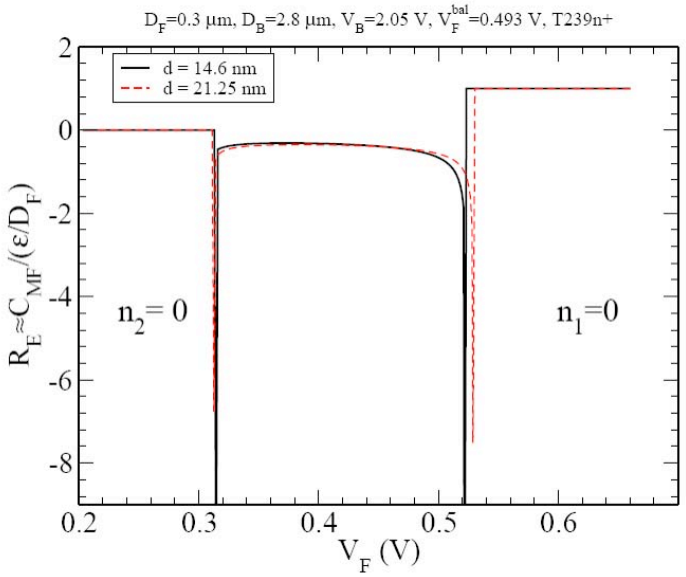

Figure 5. Calculation of the Eisenstein ratio versus front gate voltage.
The solid line is the calculation in the 2D model and the dashed line is the calculation with finite-thickness effects included, which soften the abrupt transitions

and the front gate, respectively, and we have used the approximation of uniform electric fields and Gauss's Law relate the electric fields to the charge densities. When the back-gate voltage is held fixed and the front-gate voltage is varied, then the Eisenstein ratio can be approximated as

$$R_E \approx \frac{s_1}{d + s_1 + s_2}, \tag{19}$$

where d is the effective separation of the layers (as fit to the experimental data of Ref. 5), and $s_j(n_j)$ (j =1,2) are the thermodynamic lengths of layer 1 and layer 2. The thermodynamic lengths are calculated using Eq. (10) for the 2DEG case, and with the correction in Eq. (13) for the finite-thickness case.

Figure 5 (above), is a calculation of the Eisenstein ratio for the bilayer sample of Ref. 5. There are two discontinuities in the Eisenstein ratio at $V_F \sim 0.32$ V and $V_F \sim 0.54$ V. The discontinuities are due to the monolayer-to-bilayer transition at $V_F \sim 0.32$ V and the bilayer-to-monolayer transition at $V_F \sim 0.54$ V, which are abrupt in the Hartree-Fock approximation. Finite-thickness corrections and disorder soften the abrupt layer transitions, so the

corrections would also be expected to smooth out the magnitudes of the discontinuities in the Eisenstein ratio, which is what we find in our calculations.

Finally, we calculate the interlayer capacitance per area C_{MM} as a function of the interlayer voltage V_M. When both layers are occupied, the interlayer capacitance can be expressed as

$$\frac{C_{MM}}{\varepsilon / d} = \frac{1}{\varepsilon / d}\left(\frac{d\left(n_F - n_1\right)}{dV_M}\right)_{V_F, V_B} \approx \frac{d}{d + s_1 + s_2}, \tag{20}$$

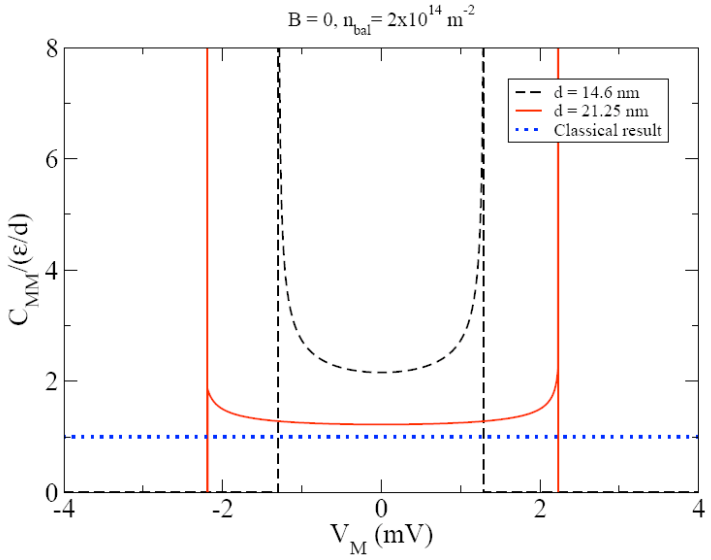

Figure 6. Interlayer capacitance per area $C_{MM} \approx \varepsilon/(d+s)$, in units of the classical result ε/d. The solid line corresponds to the calculation with finite-thickness effects included, while the dashed line shows the interlayer capacitance for zero thickness. The dotted line is the classical ($s = 0$) result, ε/d.

where all quantities are defined the same as in the calculation of the Eisenstein ratio. When either layer is empty then the larger separation distance between the other layer and the front (back) gate make the interlayer capacitance effectively zero. Figure 6 (above) is a calculation of the interlayer capacitance based on the theoretical fit to the experimental data of Ref. 5. When finite-thickness corrections are included, the effective separation d is larger which lowers the value for the interlayer capacitance. This same effect also allows for a larger voltage range for V_M.

Discussion

We presented a calculation of the Eisenstein ratio that showed a softening of the discontinuities at the monolayer-to-bilayer transition and the bilayer-to-monolayer transition. This was expected since the finite-thickness corrections softened the layer transitions when the model was fit to the data of Ref 5. Including the finite-thickness effects also had an appreciable effect on the interlayer capacitance. The capacitance was lowered as a consequence of the wave functions being "pushed apart" since they have an additional freedom to explore. This gave a higher value for the effective interlayer distance, driving down the interlayer capacitance. However, the range on interlayer voltage was increased, this is to be expected since differential capacitance is defined as $C = dQ/dV$, and a decrease in capacitance corresponds to increase in voltage, if charge is conserved, as it is in our model.

By extending previous 2DEG models with corrections based on finite-thickness we were able to improve the models agreement with experiment. These results indicate that finite-thickness effects are important in modeling the physics of bilayer devices. For future work, we plan on expanding the results of this paper by allowing more variational freedom in the minimization of the energy per area. This would include relaxing the mirror symmetry restriction that is currently in place and allow the parameters of each well, such as wave function location and form, to vary independently. It would be interesting to see if doing so could yield new insights into the models of double-quantum-well systems.

Acknowledgements

The author would like to thank Professor Charles Hanna, the staff of the McNair scholars program (David Hall, Helen Barnes, and Greg Martinez), and especially his parents, John and Nancy Durrant, for all their mentoring and support.

References

[1] J. P. Eisenstein, L. N. Pfeiffer, and K. W. West, Phys. Rev. Lett. **68**, 674 (1992).
[2] J. P. Eisenstein, L. N. Pfeiffer, and K. W. West, Phys. Rev. B **50**, 1760 (1994).
[3] T. Jungwirth and A. H. MacDonald, Phys. Rev. B **84**, 5808 (1996).
[4] C. B. Hanna, D. Haas, and J. C. Diaz-Velez, Phys. Rev. B **61**, 13882 (2000).
[5] W. R. Clarke, A. P. Micolich, A. R. Hamilton, et al., Phys. Rev. B **71**, 081304(R) (2005).
[6] A. R. Hamilton, M. Y. Simmons, C. B. Hanna, et al., Physica E **12**, 304 (2002).
[7] C. B. Hanna, (Private Communication) (2007-2008).
[8] P. P. Ruden and Z. Wu, Phys. Rev. Lett. **59**, 2165 (1991).
[9] H. C. A. Oji, A. H. MacDonald, and S. M. Girvin, Phys. Rev. Lett. **58**, 824 (1987).
[10] F. C. Zhang and S. D. Sarma, Phys. Rev. B **33**, 2903 (1986).